POLITECNICO DI TORINO
Repository ISTITUZIONALE

Optimal Energy Saving Adaptive Cruise Control in Overtaking Scenarios for a Hybrid Electric Vehicle

Original
Optimal Energy Saving Adaptive Cruise Control in Overtaking Scenarios for a Hybrid Electric Vehicle / Anselma, Pier Giuseppe; Lou, Waiyuntian; Emadi, Ali; Belingardi, Giovanni. - (2022), pp. 341-346. (Intervento presentato al convegno 2022 IEEE 31st International Symposium on Industrial Electronics (ISIE) tenutosi a Anchorage, AK, USA nel 01-03 June 2022) [10.1109/ISIE51582.2022.9831720].

Availability:
This version is available at: 11583/2970340 since: 2022-07-28T09:09:07Z

Publisher:
IEEE

Published
DOI:10.1109/ISIE51582.2022.9831720

Terms of use:

This article is made available under terms and conditions as specified in the corresponding bibliographic description in the repository

Publisher copyright
IEEE postprint/Author's Accepted Manuscript

©2022 IEEE. Personal use of this material is permitted. Permission from IEEE must be obtained for all other uses, in any current or future media, including reprinting/republishing this material for advertising or promotional purposes, creating new collecting works, for resale or lists, or reuse of any copyrighted component of this work in other works.

(Article begins on next page)

23 February 2024

POLITECNICO DI TORINO
Repository ISTITUZIONALE

Optimal Energy Saving Adaptive Cruise Control in Overtaking Scenarios for a Hybrid Electric Vehicle

Optimal Energy Saving Adaptive Cruise Control in Overtaking Scenarios for a Hybrid Electric Vehicle / Anselma, Pier Giuseppe; Lou, Waiyuntian; Emadi, Ali; Belingardi, Giovanni. - (2022), pp. 341-346. (Intervento presentato al convegno 2022 IEEE 31st International Symposium on Industrial Electronics (ISIE) tenutosi a Anchorage, AK, USA nel 01-03 June 2022) [10.1109/ISIE51582.2022.9831720].

This version is available at: 11583/2970340 since: 2022-07-28T09:09:07Z

IEEE

DOI:10.1109/ISIE51582.2022.9831720

This article is made available under terms and conditions as specified in the corresponding bibliographic description in the repository

IEEE postprint/Authors Accepted Manuscript

2022 IEEE. Personal use of this material is permitted. Permission from IEEE must be obtained for all other uses, in any current or future media, including reprinting/republishing this material for advertising or promotional purposes, creating new collecting works, for resale or lists, or reuse of any copyrighted component of this work in other works.

(Article begins on next page)

23 February 2024

problem in an off-line simulation approach. The rest of this paper is arranged as follows. First, the ACC overtaking scenario under analysis is presented. A HEV powertrain is consequently modelled. Then, DP is implemented to solve the optimal speed trajectory problem in different ACC overtaking scenarios. Simulation results are then discussed and the performance of the proposed energy-efficient ACC overtaking approach is verified. Finally, results and conclusions are given.

II. ACC Overtaking Scenario

A schematic diagram of the ACC overtaking scenario studied in this paper is illustrated in Fig. 1. Initially, both Following Vehicle and Leader Vehicle travel with the same speed as the queue of vehicles ahead, hereafter denoted as initial speed. The Leader Vehicle then decides to overtake the queue of vehicles and accelerates up to a certain speed, hereafter denoted as target speed. In this framework, the automated Following Vehicle needs to plan the longitudinal speed trajectory to appropriately follow the Leader Vehicle. The overall overtaking scenario can be divided into three phases. In the first phase, the Leader Vehicle performs the lane change maneuver while accelerating up to the target speed. The queue of low-speed vehicles is overtaken in a reduced amount of time during the second phase. In the third phase, the Leader Vehicle performs another lane change maneuver and returns to the original road lane. In the first and third phases, the lateral velocity planning problem for the lane change maneuvers in Fig. 1 can be addressed using different approaches (e.g. the polynomial method [12]). On the other hand, this paper focuses on the longitudinal speed planning problem for the overall ACC overtaking scenario.

During phase 1 in Fig. 1, the Following Vehicle needs to adjust its speed and follow the Leader Vehicle while it accelerates to overtake the queue of slow speed vehicles. In the first time instant (i.e. $t = t_0$), initial values are set for the Following Vehicle longitudinal speed, the Leader Vehicle longitudinal speed and initial inter-vehicular distance (IVD) d_0. Both vehicles are assumed travelling at the same speed as the queue of slow speed vehicles in the first time instant. In the final time instant (i.e. $t = t_{end}$), both vehicles will get to a known final state characterized by the value of Following Vehicle longitudinal speed being comparable with the value of the Leader Vehicle longitudinal speed (i.e. the target speed) and by a certain IVD d_{end}. Several requirements need to be satisfied for the longitudinal speed trajectory generated over time for the Following Vehicle. First, the collision between the Following Vehicle and the Leader Vehicle must be avoided. Second, the instantaneous values of longitudinal speed and acceleration of the Following Vehicle should not exceed the respective vehicle operational constraints. Third, passenger comfort, maneuver efficiency (i.e. the time required to complete the overtaking maneuver), and HEV energy economy should be maximized. Nevertheless, these requirements are usually contradictory. For example, an aggressive longitudinal acceleration leads to improve the maneuver efficiency, yet it comes at the expense of worsening both the passenger comfort and the energy economy.

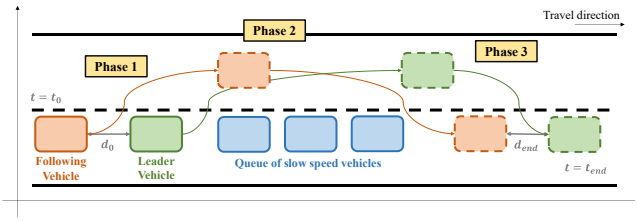

Fig. 1. ACC overtaking scenario.

III. HEV Powertrain Modelling and Control

This section describes the implemented numerical approach to evaluate the energy consumption of the HEV retained as Following Vehicle in the considered ACC overtaking scenario. The HEV powertrain architecture and its hybrid supervisory control logic are detailed to this end.

A. HEV Powertrain

A prototype Chevrolet Blazer is investigated as HEV in this study. The electrified Blazer is the McMaster University's vehicle for the US Department of Energy sponsored EcoCAR4 competition. The electrified Blazer prototype is designed to compete with its traditional version which is propelled by an internal combustion engine (ICE) alone.

Fig. 2 shows a schematic diagram of the electrified Blazer powertrain, which relates to a parallel-through-the-road P0-P4 configuration. The HEV is equipped with a 1.5L 171kW turbocharged spark-ignition ICE and a Valeo i-StARS 4kW Belt Alternator Starter (BAS) directly connected with the ICE shaft in P0 position. During ICE cranking events, the BAS drives the engine crank shaft. When the ICE is activated, the BAS generates an auxiliary torque that can be either negative or positive to adjust the engine torque to its optimal efficiency region. The BAS is connected to a 12V battery which powers the low voltage vehicle accessories. Both ICE and BAS propel the front axle through a nine-speed automatic transmission (AT). On the other hand, the rear axle is connected to a YASA P400 300V 90kW electric motor/generator (EM) in P4 position through a final drive (FD) and a clutch. When the YASA P400 EM is not operating, the related clutch is disengaged to avoid drag losses of the EM. The YASA P400 EM is linked to a 300V 52kW 1.5kWh GM Malibu Hybrid battery pack which serves as high-voltage energy storage system (ESS). Separating high-voltage electrical systems from low-voltage electrical systems was found to be beneficial for HEV fuel economy. In this case, electrical energy harvested during braking events by the YASA P400 EM is

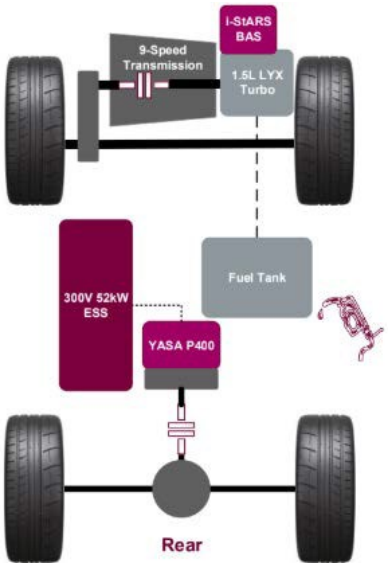

Fig. 2. Schematic diagram of the McMaster EcoCAR4 Team's P0-P4 electrified Blazer powertrain.

used for operating the rear axle instead of supplying the vehicle low-voltage electrical loads [13].

In general, the HEV is modelled here according to the widely adopted quasi-static approach [14]. At each time instant, the torque at the wheels T_{wheels} can be expressed as a function of the road slope α, the longitudinal vehicle speed V, and the commanded vehicle longitudinal acceleration a_x as follows:

$$T_{wheels} = \left\{m \cdot g \cdot cos(\alpha) \cdot (f_0 + k \cdot V^2) + \frac{1}{2} \cdot \rho \cdot V^2 \cdot S \cdot C_x + m \cdot g \cdot sin(\alpha) + m_{equ} \cdot a_x\right\} \cdot r_{wheel} \quad (1)$$

where m, g and ρ stand for the vehicle mass, the gravitational acceleration, and the air density, respectively. C_x is the aerodynamic drag coefficient in the longitudinal direction. f_0 and k denote rolling resistance coefficients. S, r_{wheel} and m_{equ} are the vehicle frontal area, the wheel dynamic radius, and the equivalent vehicle mass including the inertia of rotating components as well.

Speeds of power components can be directly evaluated from the vehicle speed. Moreover, the torque balance at the wheels in each time instant can be expressed as follows:

$$T_{wheels} = \left[T_{ICE} + T_{BAS} \cdot \tau_{belt} \cdot \eta_{belt}^{sign(T_{BAS})}\right] \cdot \tau_{AT}(gear) \cdot \tau_{FD-front} \cdot \eta_{AT} \cdot \eta_{FD-front} + T_{EM} \cdot \tau_{FD-rear} \cdot \eta_{FD-rear}^{sign(T_{EM})} \quad (2)$$

where T_{ICE}, T_{BAS} and T_{EM} are the ICE torque, the BAS torque, and the EM torque, respectively. Ratios of the belt connecting BAS with ICE, of the engaged gear in the AT, of the front axle FD and of the rear axle FD are respectively denoted by τ_{belt}, $\tau_{AT}(gear)$, $\tau_{FD-front}$ and $\tau_{FD-rear}$. Finally, η_{belt}, η_{AT}, $\eta_{FD-front}$, and $\eta_{FD-rear}$ stand for mechanical efficiencies of the belt, the AT, the FD of the front axle and the FD of the rear axle, respectively. Considering the sign of the torques of BAS and EM as power factors of respective efficiencies for the belt and for the rear FD allows retaining both propelling and generating cases for the electric machines.

The electrical power values of the 12V battery and of the 300V ESS can be determined by interpolating in two-dimensional lookup tables that map the electrical power consumption of the BAS and of the EM, respectively, as a function of their speed and torque. Low-voltage auxiliary loads are considered as well for the 12V battery connected to the BAS. The instantaneous values of current for both 12V battery and 300V ESS can then be evaluated according to a first-order equivalent circuit model by retaining as input the respective electrical power. Finally, values of state-of-charge (SOC) for both 12V battery and 300V ESS are determined by integrating their current over time and by weighting according to the respective capacities.

As regards the ICE, its instantaneous fuel rate can be modelled by interpolating in a two-dimensional lookup table with speed and torque as independent variables. The interested reader can find more details regarding the implemented HEV modeling procedure in [13].

B. Hybrid Supervisory Control Logic

The hybrid supervisory controller is responsible for deciding the instantaneous torque split between power components. This is a crucial decision that affects the overall HEV energy economy. The function of the BAS is to generate a reactive torque that allows shifting the ICE operating point towards highly efficient areas. On the other hand, the torque of the EM connected to the rear axle is controlled to enable matching between the overall provided value of T_{wheels} and the corresponding driver's demand.

At each time instant, the gear shifting logic embedded in the AT selects the gear ratio to be engaged according to the current value of vehicle speed. Then, the ICE angular speed can be obtained as follows:

$$\omega_{ICE} = \frac{V \cdot \tau_{AT}(gear) \cdot \tau_{FD-front}}{r_{wheel}} \quad (3)$$

The optimal ICE torque is consequently determined by maximizing the ICE efficiency based on the current value of ω_{ICE}. However, the difference between the wheel torque command and the optimal ICE torque should be compensated by the BAS and the YASA motor. Thus, after the optimal engine torque is obtained, the compensating torque is calculated and compared with the upper and lower torque limit of the BAS. If the compensating torque is larger than the upper limit of the BAS, it means the wheel torque command is too large and ICE and BAS are not able to provide enough torque alone. The YASA motor will engage in this case and supply the rest of the propelling torque. Similarly, the YASA motor will provide a reactive torque and charge the high-voltage battery pack in case the wheel torque at the front axle exceeds the corresponding driver's demand.

Once the torque command of ICE, BAS, and YASA motor are known, the fuel mass flow rate $\dot{m}_{fuel}$, the current of the low voltage battery and the current of the high voltage battery can be determined using the motor and battery models discussed in the previous section. Evaluating the overall HEV energy consumption can be performed in this way.

IV. Optimal ACC Overtaking Planning Problem

In this section, the optimal ACC overtaking planning problem is discussed. The aim here involves minimizing the overall HEV energy consumption in the considered overtaking maneuver time horizon as follows:

$$\arg\min \left\{ \int_{t_0}^{t_{end}} \begin{bmatrix} LHV_{fuel} \cdot \dot{m}_{fuel}(t) + \\ +I_{HV}(t) \cdot OCV_{HV}(t) + \\ +I_{LV}(t) \cdot OCV_{LV}(t) \end{bmatrix} dt \right\}$$

subject to: (4)

$$IVD_{min}(t) \leq IVD(t) \leq IVD_{MAX}(t)$$

$$\left|\ddot{x}_{Following}(t)\right| \leq \left|\ddot{x}_{MAX}(t)\right|$$

where $\dot{m}_{fuel}$ and LHV_{fuel} are the fuel mass flow rate in grams per second and the fuel low heating value in joule per gram, respectively. I_{HV} and I_{LV} stand for values of current for the high-voltage battery pack and the low-voltage battery, respectively. Finally, OCV_{HV} and OCV_{LV} are the respective values of open-circuit voltage. The overall HEV power consumption can be expressed considering fuel power, high-voltage battery power and 12V battery power in watts in this way.

Two additional constraints are involved in the ACC overtaking planning problem. The first one relates to the IVD, which must always be limited within minimum and maximum values. Indeed, the Following Vehicle must both avoid colliding with the Leader Vehicle, prevent getting too far from the Leader Vehicle, and avoid colliding with the vehicles travelling at low speed during the lateral maneuver to return to the starting lane. The second optimization constraint

involves limiting the instantaneous value of Following Vehicle jerk $\ddot{x}_{Following}$ within reasonable values both to improve passenger comfort and to comply with the operational limits of the HEV powertrain components. The follow-up of this section will discuss a DP formulation that allows finding the global optimal solution for the presented ACC overtaking planning problem.

A. Dynamic Programming formulation

DP is a widely implemented approach that enables identifying global optimal control trajectories for a given dynamic control problem. DP is based on the principle of global optimality introduced by Bellman and it involves exhaustively sweeping discretized values of control and state variables of the control problem [15]. This procedure is iterated backwardly while solving an optimal control problem from the final time instant to the initial one [16]. The control variable set U and the state variable set X considered in DP for this work are reported in (5).

$$U = \{\ddot{x}_{Following}\} \quad ; \quad X = \begin{Bmatrix} IVD \\ \dot{x}_{Following} \\ \ddot{x}_{Following} \end{Bmatrix} \tag{5}$$

DP controls at each time instant the Following vehicle jerk. On the other hand, X contains the variables whose values need to be tracked over time throughout the overtaking maneuver. The longitudinal acceleration $\ddot{x}_{Following}$ and the longitudinal speed $\dot{x}_{Following}$ of the Following vehicle are considered here in X along with the IVD. Starting from the controlled value of $\ddot{x}_{Following}$, all the state variables can be updated in the generic time instant t according to the backward Euler method as follows:

$$\begin{aligned} \ddot{x}_{Following}(t+1) &= \ddot{x}_{Following}(t) \cdot \Delta t + \ddot{x}_{Following}(t) \\ \dot{x}_{Following}(t+1) &= \ddot{x}_{Following}(t) \cdot \Delta t + \dot{x}_{Following}(t) \\ IVD(t+1) &= \dot{x}_{Following}(t) \cdot \Delta t + IVD(t) \end{aligned} \tag{6}$$

where Δt is the DP simulation time step in seconds. DP explores discretized values of control and state variables in the ACC overtaking scenario to find the control solution that minimizes the cost function expressed in (4) in terms of estimated HEV power consumption. For each possible combination of control and state variables, the overall HEV energy consumption can be evaluated by following the methodology illustrated in Section II. Constraints are imposed in this framework to the values of state variables. The open-source DP function provided by Sundstrom and Guzzella and implemented in Matlab® is used in this work [17].

B. ACC algorithm assessment methodology

The performance of the proposed algorithm is assessed by following the flowchart illustrated in Fig. 3. First, initial conditions are considered in terms of longitudinal speed and position of Leader vehicle, Following Vehicle and vehicles traveling in queue at slow speed.

Step 1. The longitudinal vehicle and electrified powertrain dynamics for the Leader vehicle are simulated throughout the overtaking maneuver. In this case, the Leader vehicle is supposed embedding the electrified Blazer HEV powertrain as well. A Simulink® model is considered here that takes as input the target vehicle longitudinal speed profile over time. Then, the Simulink® model is composed by the following sub-systems: 1) a PID controller which models the driver and determines the value of vehicle acceleration required at each time instant to reproduce the target longitudinal vehicle speed profile; 2) the HEV powertrain model which allows accounting for operational limits of power components and predicting the overall HEV energy consumption; 3) a longitudinal vehicle dynamic model which allows evaluating the longitudinal position and speed of the vehicle over time considering the instantaneous values of the vehicle resistive forces and of the torque T_{wheels} provided by the HEV powertrain. The initial speed value is set in the first time instant, while the target speed is instantaneously imposed to the PID controller which models the driver when $t = 0.1$ seconds. In this case, the power capability of the HEV powertrain components will eventually restrict the maximum acceleration achievable by the simulated electrified Blazer. Here, all the vehicles are assumed traveling on a flat road. The Leader vehicle is assumed being 5 meters behind the queue of slow speed vehicles in the initial time instant t_0. Then, the simulation in Simulink® performed at Step1 is carried out until the Leader vehicle gets 15 meters ahead the queue of slow speed vehicles. This value has been assumed to allow the Following vehicle enough space to enter the lane in between the Leader vehicle and the queue of slow speed vehicles. The value of the final time instant t_{end} is determined in this way. Simulation results for the Leader vehicle in terms of longitudinal position, longitudinal speed and energy consumption over time are obtained once Step 1 is completed.

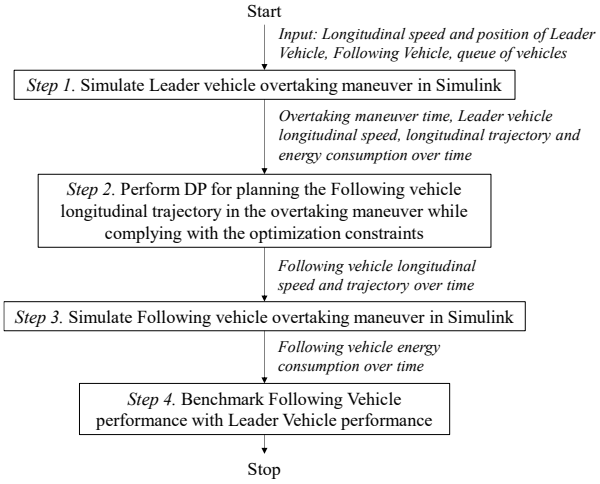

Fig. 3. Flowchart for assessing the performance of the proposed optimal ACC overtaking planning algorithm.

Step 2. Looking at Fig. 3, this step involves planning the longitudinal jerk of the Following vehicle over time throughout the overtaking maneuver by performing the DP optimization described in Section IV.A. The longitudinal trajectory of the Leader vehicle determined in Step 1 is used in this case to evaluate the IVD at each simulation time instant and thus constrain it within allowed limits. In DP, IVD_{min} over time is evaluated here according to a time-headway numerical braking model with Following Vehicle speed and relative vehicle speed between Leader Vehicle and Following Vehicle as inputs. More details regarding this procedure can be found in [6]. On the other hand, IVD_{MAX} is assumed here being 30 meters. The initial IVD is set to 10 meters, while the final value of IVD is constrained in DP to be within 3 meters and the initial IVD to ensure that both Leader Vehicle and Following Vehicle travel approximately the same distance. Concerning $\ddot{x}_{MAX}$, its value has been set here to 10 m/s^3 as the

threshold for reasonable passenger comfort [18]. Here, the DP simulation time step Δt is set to 0.1 seconds.

Step 3. The Following vehicle longitudinal speed over time evaluated by DP is fed as input to the same HEV Simulink® model used in Step 1. This allows evaluating the energy consumption of the Following vehicle according to the same numerical platform as for the Leader vehicle. Finally, obtained results for the proposed optimal energy saving ACC overtaking planning algorithm are analyzed in Step 4.

V. Results

This section illustrates the results obtained by the proposed DP formulation for solving the optimal ACC overtaking planning problem. In particular, the flowchart illustrated in Fig. 3 is repeated considering different initial conditions in terms of initial speed and target speed (i.e. the overtaking speed). Looking at Fig. 1, both Leader Vehicle, Following Vehicle and slow speed vehicles are assumed traveling at the same speed in the initial time instant. Five test cases are retained here with corresponding values of initial speed and target speed reported in Table I. The time required to complete each overtaking maneuver as calculated during Step 1 in Fig. 3 is reported as well. The HEV energy consumption in watt-hour per kilometer of driving in Table I includes both fuel consumption, 12V battery energy consumption and high-voltage battery pack energy consumption. The effectiveness

TABLE I. Simulation Results for the Retained Overtaking Scenarios

Test case #	Initial speed [km/h]	Target speed [km/h]	Over-take time [s]	Energy consumption - L [Wh/km]	Energy consumption - F [Wh/km]	Road and inertia loss [kJ]		ICE loss [kJ]		12V loss [kJ]		300V loss [kJ]	
						L	F	L	F	L	F	L	F
1	50	70	6.81	0.97	0.96 (-1.8%)	223	224	99	96	37	29	318	305
2	50	80	5.74	1.43	1.38 (-3.6%)	310	298	84	84	24	24	495	468
3	60	80	6.50	1.11	1.08 (-2.1%)	268	273	125	124	37	33	398	367
4	60	90	5.87	1.49	1.43 (-4.1%)	378	361	112	111	25	24	589	548
5	70	90	6.87	1.16	1.14 (-1.2%)	322	337	178	175	38	32	450	431

[a] L=Leader ; F=Following

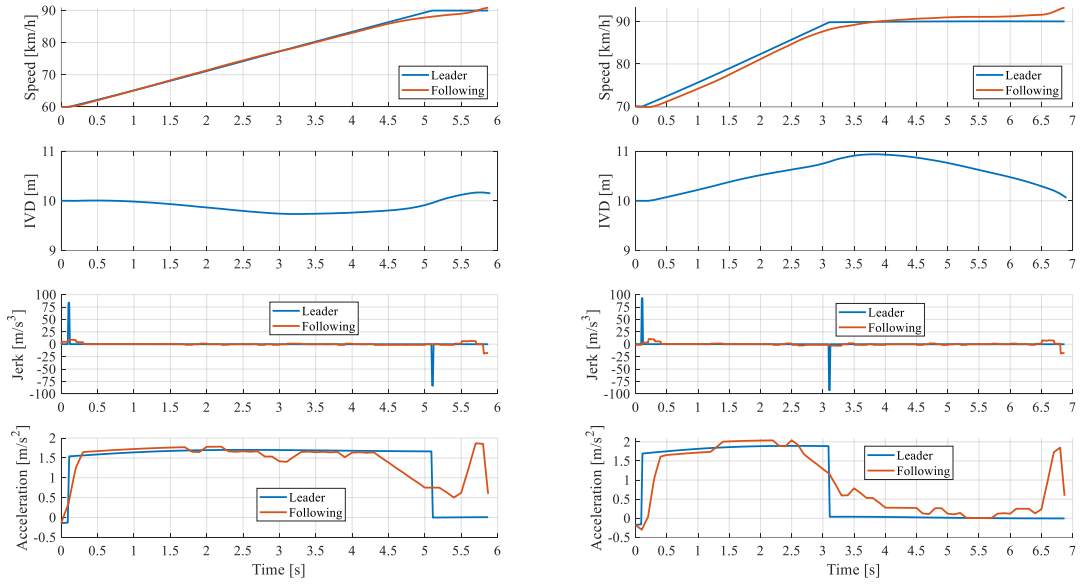

(a) Test case #2 (b) Test case #5

Fig. 4. Time series of longitudinal speed, IVD, longitudinal jerk and logitudinal acceleration for both Leader Vehicle and Following Vehicle in the ACC overtaking scenarios corresponding to test cases #2 and #5.

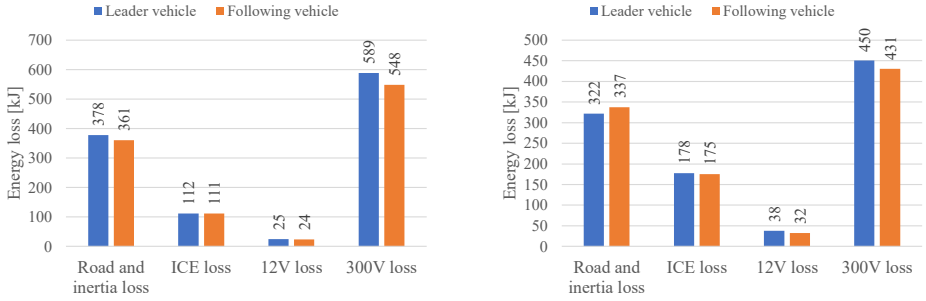

(a) Test case #2 (b) Test case #5

Fig. 5. Breakdown of the HEV powertrain losses in the overtaking scenarios corresponding to test cases #2 and #5.

of the proposed optimal ACC overtaking planning algorithm is demonstrated by the significant improvements in terms of overall HEV energy economy for the Following Vehicle compared with the Leader Vehicle. Maximum potential energy saving relates to the test cases with more aggressive Leader Vehicle acceleration (i.e. test case #2 and test case #4) and amount to 3.6% and 4.1%, respectively.

Fig. 4 shows examples of time series for both Leader Vehicle and Following Vehicle controlled by the proposed DP based optimal ACC overtaking planning algorithm in test cases #2 and #5. As it can be noticed, remarkable smoothing of the vehicle longitudinal jerk can be achieved for the Following Vehicle compared with the Leader Vehicle. Lower values of longitudinal jerk consequently entail more uniform vehicle acceleration and vehicle speed as well, which is beneficial for HEV energy economy. The remarkable potential in terms of passenger comfort improvement brought by the introduced ACC overtaking algorithm is thus demonstrated. The slight acceleration comebacks towards the end of the overtaking maneuvers both in Fig. 4(a) and in Fig. 4(b) can be explained by the compliance of the longitudinal speed profile planned by DP with the optimization constraint imposed on the final IVD.

Table I also reports the breakdown of the HEV powertrain losses for both Leader Vehicle and Following. In particular, the road and inertia loss can be obtained by multiplying T_{wheels} times the wheel angular speed. The ICE loss can be determined by subtracting the ICE mechanical power from the fuel power. Finally, 12V loss and 300V loss terms are evaluated by comparing the electric machine mechanical power with the battery electrical power for BAS/12V battery and for EM/high-voltage battery pack, respectively. Fig. 5 illustrates a graphical representation of the breakdown of HEV powertrain losses for the overtaking scenarios corresponding to test cases #2 and #5, respectively. In Fig. 5 (a), one of the major contributors to the energy saving of the Following Vehicle compared with the Leader Vehicle relate to the decrease in road and inertia loss which can be obtained by smoothing the profile of the longitudinal speed over time. Both in Fig. 5(a) and in Fig. 5(b), a significant reduction in the loss of the high-voltage EM and battery pack can be achieved as well thanks to the proposed optimal ACC overtaking planning algorithm. As shown in Fig. 5(b), DP unexpectedly chooses to increase road and inertia loss of the Following Vehicle in test case #5. Nevertheless, HEV energy saving in the overtaking maneuver can still be ensured by consistently lowering both ICE loss, 12V loss, and 300V loss.

VI. Conclusions

The longitudinal speed trajectory over time during overtaking scenarios has a large impact on both passenger comfort and HEV energy economy. In this paper, an optimization method is adopted to off-line solve the longitudinal speed planning problem for an HEV travelling as Following Vehicle in ACC overtaking scenarios. DP is implemented as global optimal control approach, and the optimization target includes maximizing the overall HEV energy economy while limiting the longitudinal vehicle jerk. Constraints are considered as well for longitudinal dynamics of the Following Vehicle and for the safety distance between the Following Vehicle and the Leader Vehicle. Simulation results are obtained in different ACC overtaking scenarios considering the McMaster University's electrified Blazer as test HEV. The introduced DP based optimal ACC overtaking planning algorithm can significantly smooth the longitudinal jerk of the Following Vehicle in overtaking maneuvers, thus enhancing passenger comfort. Moreover, up to 4.1% energy saving can be achieved by the Following Vehicle compared with the Leader Vehicle. Related future work can involve developing and implementing a real-time capable ACC overtaking planning algorithm based on the off-line optimized control trajectories obtained in this work.

References

[1] N. F. Hutchins, A. J. Kerr and L. R. Hook, "User Acceptance in Autonomous Vehicles: The Evolution of the End User," *2019 International Symposium on Systems Engineering (ISSE)*, 2019, pp. 1-8.

[2] A. Rasouli and J. K. Tsotsos, "Autonomous Vehicles That Interact With Pedestrians: A Survey of Theory and Practice," in *IEEE Transactions on Intelligent Transportation Systems*, vol. 21, no. 3, pp. 900-918, March 2020.

[3] J. Pauwelussen and P. J. Feenstra, "Driver Behavior Analysis During ACC Activation and Deactivation in a Real Traffic Environment," in *IEEE Transactions on Intelligent Transportation Systems*, vol. 11, no. 2, pp. 329-338, June 2010.

[4] P. Shakouri, A. Ordys, D.S. Laila, M. Askari, "Adaptive cruise control system: comparing gain-scheduling PI and LQ controllers", *IFAC Proceedings Volumes*, vol. 44, no. 1, pp. 12964-12969, 2011.

[5] D. Moser, R. Schmied, H. Waschl and L. del Re, "Flexible Spacing Adaptive Cruise Control Using Stochastic Model Predictive Control," in *IEEE Transactions on Control Systems Technology*, vol. 26, no. 1, pp. 114-127, Jan. 2018.

[6] P.G. Anselma, "Optimization-Driven Powertrain-Oriented Adaptive Cruise Control to Improve Energy Saving and Passenger Comfort", *Energies*, vol. 14, no. 10, pp. 2897-2924, 2021.

[7] M. Althoff, S. Maierhofer and C. Pek, "Provably-Correct and Comfortable Adaptive Cruise Control," in *IEEE Transactions on Intelligent Vehicles*, vol. 6, no. 1, pp. 159-174, March 2021.

[8] A. Capuano, M. Spano, A. Musa, G. Toscano, D. Misul, "Development of an Adaptive Model Predictive Control for Platooning Safety in Battery Electric Vehicles", *Energies*, vol. 14, no. 17, pp. 5291-5304, 2021.

[9] D. Kim, S. Moon, J. Park, H. J. Kim and K. Yi, "Design of an Adaptive Cruise Control / Collision Avoidance with lane change support for vehicle autonomous driving," *2009 ICCAS-SICE*, 2009, pp. 2938-2943.

[10] R. Dang, J. Wang, S. E. Li and K. Li, "Coordinated Adaptive Cruise Control System With Lane-Change Assistance," in *IEEE Transactions on Intelligent Transportation Systems*, vol. 16, no. 5, pp. 2373-2383, Oct. 2015.

[11] K.W. Schmidt, "Cooperative adaptive cruise control for vehicle following during lane changes", *IFAC-PapersOnLine*, vol. 50, no. 1, pp. 12582-12587, 2017.

[12] G. Xu, L. Liu, Y. Ou and Z. Song, "Dynamic Modeling of Driver Control Strategy of Lane-Change Behavior and Trajectory Planning for Collision Prediction," in *IEEE Transactions on Intelligent Transportation Systems*, vol. 13, no. 3, pp. 1138-1155, Sept. 2012.

[13] M. Haußmann, "Development of a Control System for a P4 Parallel-Through-The-Road Hybrid Electric Vehicle", *M.Sc. Thesis, McMaster University*, 2019.

[14] G. Rizzoni, L. Guzzella and B. M. Baumann, "Unified modeling of hybrid electric vehicle drivetrains," in *IEEE/ASME Transactions on Mechatronics*, vol. 4, no. 3, pp. 246-257, Sept. 1999.

[15] R. Bellman and E. Lee, "History and development of dynamic programming," in *IEEE Control Systems Magazine*, vol. 4, no. 4, pp. 24-28, November 1984.

[16] F. Miretti, D. Misul, D., E. Spessa, "DynaProg: Deterministic Dynamic Programming solver for finite horizon multi-stage decision problems", *SoftwareX*, vol. 14, p. 100690, 2021.

[17] O. Sundstrom and L. Guzzella, "A generic dynamic programming Matlab function," *2009 IEEE Control Applications, (CCA) & Intelligent Control, (ISIC)*, 2009, pp. 1625-1630.

[18] Q. Huang, H. Wang, "Fundamental Study of Jerk: Evaluation of Shift Quality and Ride Comfort", *SAE Technical Paper* 2004-01-2065, 2004.